



1 Effect of land-sea air masses transport on spatiotemporal distributions of atmospheric CO₂
2 and CH₄ mixing ratios over the south Yellow Sea

3 Jiaxin Li¹, Kunpeng Zang^{1,2,3*}, Yi Lin¹, Yuanyuan Chen¹, Shuo Liu¹, Shanshan Qiu¹, Kai Jiang
4 ¹, Xuemei Qing¹, Haoyu Xiong¹, Haixiang Hong¹, Shuangxi Fang^{2,4*}

5 ¹ *College of Environmental and Resources Sciences, Zhejiang University of Technology, Hangzhou,*
6 *China, ² Zhejiang Carbon Neutral Innovation Institute, Zhejiang University of Technology,*
7 *Hangzhou, China, ³ National Marine Environmental Monitoring Center, Dalian, China,*
8 ⁴ *Collaborative Innovation Center on Forecast and Evaluation of Meteorological Disasters (CIC-*
9 *FEMD), Nanjing University of Information Science & Technology, Nanjing, China*

10 **Corresponding to:** Kunpeng Zang (zangkunpeng@zjut.edu.cn), Shuangxi Fang
11 (fangsx@zjut.edu.cn)

12
13 **Abstract:** To reveal the spatiotemporal distributions of atmospheric CO₂ and CH₄ mixing ratios
14 and regulation mechanisms over the China shelf sea, two field surveys were conducted in the south
15 Yellow Sea in China in November 2012 and June 2013, respectively. Observed results showed that
16 mean atmospheric CO₂ and CH₄ mixing ratios were 403.50 ± 13.70 ppm and 1934.1 ± 33.6 ppb in
17 November 2012, and 396.40 ± 12.30 ppm and 1919.2 ± 30.2 ppb in June 2013, respectively. An
18 improved data filtering method were established to flag diverse sources of atmospheric CO₂ and
19 CH₄ in survey area. We found that, compared to the influences of air-sea exchange, the
20 spatiotemporal distributions of atmospheric CO₂ and CH₄ mixing ratios over the south Yellow Sea
21 were dominated by land-sea air masses transport, which was driven by seasonal monsoon. In
22 addition, atmospheric CO₂ and CH₄ mixing ratios over the south Yellow Sea could be elevated
23 remarkably in a distance of approximate 20 km offshore by land-to-sea air masses transportation
24 from the Asia Continent during early winter monsoon.

25 **Keywords:** carbon dioxide, methane, monsoon, marine boundary air, shipborne underway
26 measurement.



1 Introduction

2 Carbon dioxide (CO₂) and methane (CH₄) are the two most important greenhouse gases,
3 playing critical roles in Earth's radiation balance (AGGI, 2014). Since the industrial revolution era
4 (~1750), atmospheric CO₂ and CH₄ mixing ratios have increased and reached their highest values
5 of 415.7 ± 0.1 ppm and 1908 ± 2 ppb in 2021, which were about 149% and 262% of the preindustrial
6 levels (WMO greenhouse gas bulletin, 2022). Increasing of atmospheric CO₂ and CH₄ was
7 unequivocally attributed to anthropogenic emissions, e.g., industrial production, deforestation,
8 fossil fuel consumption (Houghton, 2003; Peters et al., 2012), and natural source-sink processes
9 (Zang et al., 2017).

10 For decades, increasing CO₂ and CH₄ mixing ratios have attracted more and more attention
11 from science community. According to the observation platforms or methods, shipborne observation
12 was considered as one of six common and important methods for studying the greenhouse gases
13 (Matsueda et al., 1996; Daube et al., 2002; Dlugokencky et al., 2005; Crosson, 2008; Fang et al.,
14 2015). Based on shipborne discrete sampling and measurement, latitudinal distribution of CH₄
15 mixing ratio with a shape drop in the area of 20 °N in marine boundary air of the North Pacific
16 Ocean were reported, which was mainly influenced by air masses transportation driven by both
17 winter monsoon and trade wind (Matsueda et al., 1996; Dlugokencky et al., 2005). In coastal area
18 of the Bohai Sea, seasonal variations of atmospheric CO₂, CH₄ and N₂O mixing ratios were mainly
19 influenced by land-sea air masses transportation based on discrete sampling observation (Kong et
20 al., 2010). Moreover, periodic observed CO₂ and CH₄ mixing ratios in marine boundary air were
21 also used to improve the accuracy of calculated air-sea CO₂ flux in the northern South China Sea
22 and the Luzon Strait (Zhai et al., 2015), and assess impacts of several episodic oil and gas spill
23 events on abnormal air-sea CH₄ flux in the Bohai Sea (Zhang et al., 2014).

24 In recent years, high-accuracy shipborne continuous observation method has been developed
25 and applied to observe greenhouse gases in marine boundary air (Nara et al., 2014; Zang et al., 2017;
26 Reddick et al., 2019), which could reveal more detailed information associated with their source-
27 sink processes. Latitudinal distributions of both CO₂ and CH₄ mixing ratios in the China shelf sea
28 boundary air in early spring were observed, which were similar to that in the north Pacific Ocean
29 (Matsueda et al., 1996; Zang et al., 2017), and mainly impacted by atmospheric chemical processes,



1 air-sea interaction in Yangtze River estuary area and land-sea air masses transportation (Zang et al.,
2 2017; Liu et al., 2018). Meanwhile, as important anthropogenic hot spot sources of atmospheric
3 CO₂ and CH₄, oil and gas platforms in global oceans were paid more attention currently. Peak values
4 of CO₂ and CH₄ mixing ratios in downwind area of oil and gas platforms were observed by
5 shipborne continuously measurement systems in the North Sea, the South China Sea and Bohai Sea.
6 Combined with the Gaussian plume model, CH₄ emissions could be quantified via “top-down”
7 approach (Nara et al., 2014; Riddick et al., 2019; Zang et al., 2020; Jia et al., 2022).

8 Monsoon is a kind of climatic phenomenon in which the dominant wind system changes with
9 seasons (Lyu et al., 2021). The East Asian monsoon (EAM), comprising the East Asian summer
10 monsoon (EASM) and East Asian winter monsoon (EAWM), is an important component of the
11 Earth’s climate system and has a significant influence on the socioeconomic, agricultural and
12 cultural development of East Asia (Huang, 1985; Zou et al., 2018; Lyu, et al., 2021). Previous studies
13 have shown that the Asian monsoons played an important role in the global and regional climate
14 variability (Huang, 1985; Chang et al., 2000; Ding et al., 2007; Zhan and Li, 2008). On the one hand,
15 spatiotemporal distributions of CO₂ and CH₄ in marine boundary air were influenced by multiple
16 processes, such as land-sea air masses transport (Bartlett et al., 2003; Zang et al., 2017), ship
17 emission (Warneke et al., 2005; Law et al., 2013; Bouman et al., 2017; Ding et al., 2018) and oil
18 and gas platforms (Nara et al., 2014; Reddick et al., 2019; Zang et al., 2020). On the other hand,
19 greenhouse gases have been observed and studied in East Asia and Pacific Ocean based on land
20 (island)-based stations (Fang et al., 2015; 2017; Luan et al., 2016), ship and plane observation
21 platforms (Matsueda et al., 1996; Bartlett et al., 2003; Dlugokencky et al., 2005). However, as an
22 important pathway of atmospheric components transportation between the Asia Continent and
23 Pacific Ocean, spatiotemporal distributions and regulate mechanisms of CO₂ and CH₄ in the China
24 shelf seas boundary air were still rare (Zhang et al., 2007; Zang et al., 2017; Liu et al., 2018).

25 In this study, atmospheric CO₂ and CH₄ mixing ratios in boundary air of the South Yellow Sea
26 (SYS) were simultaneously observed by a self-assembled shipborne CRDS (Cavity Ring-down
27 Spectroscopy, Picarro G2301, USA) system in November 2012 and June 2013, when typical periods
28 of the EASM and the EAWM. The major objects of this work were (1) to optimize an improved data
29 filter approach for shipborne underway continuous observed atmospheric CO₂ and CH₄ mixing

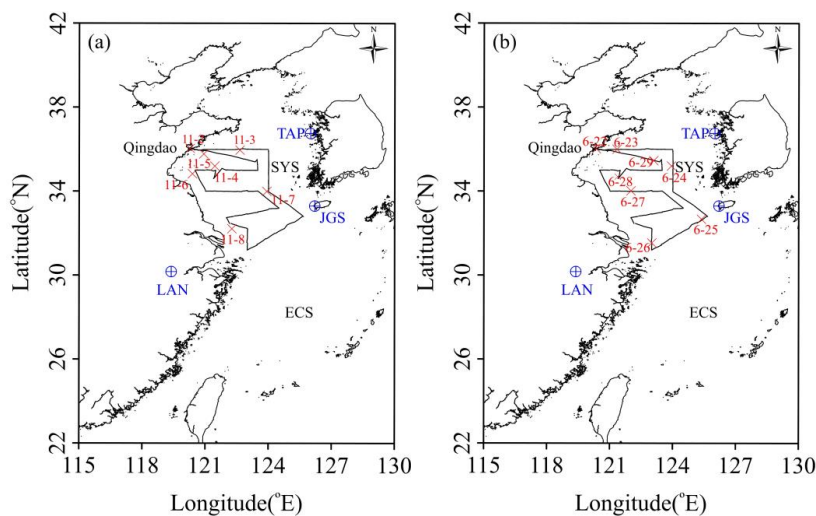


1 ratios, (2) to investigate the influence of air-sea exchange on the spatiotemporal distributions of CO₂
2 and CH₄ mixing ratios in boundary air of the SYS, and (3) to reveal the regulating mechanism of
3 seasonal monsoon on spatiotemporal distributions of CO₂ and CH₄ in boundary air of the SYS
4 during the field surveys.

5 2 Method and materials

6 2.1 Observation area

7 The Yellow Sea is a semi-enclosed marginal sea, located on the western part of the Pacific
8 Ocean, adjacent by China to the north and west, and Korean Peninsula to the east (Zhang and Chu,
9 2018; Wang et al., 2021). It is a main pathway of air mass transport between the Asia continent and
10 Pacific Ocean, and can be divided into two basins: the North Yellow Sea (NYS) and the SYS (Lyu
11 et al., 2021). The SYS covers an area of about 10.8×10^4 km², with an average depth of 44 m, and is
12 strongly influenced by the EAM system (Zou et al., 2018). As showed in Fig. 1, to study the
13 distributions of atmospheric CO₂ and CH₄ mixing ratios and their regulation mechanisms, two
14 campaigns were conducted from 2nd to 8th November, 2012 and from 22nd to 29th June, 2013,
15 respectively, both of which were typical periods of the EAM (including summer monsoon and
16 winter monsoon). In order to ensure the comparability of observations, parallel observed CO₂ and
17 CH₄ data from the three ground stations (LAN, JGS, TAP) in vicinity of the study area, were
18 presented and studied in this study.



19
20 Fig. 1. Observation area in the SYS. The thick solid black lines represent cruise tracks in November

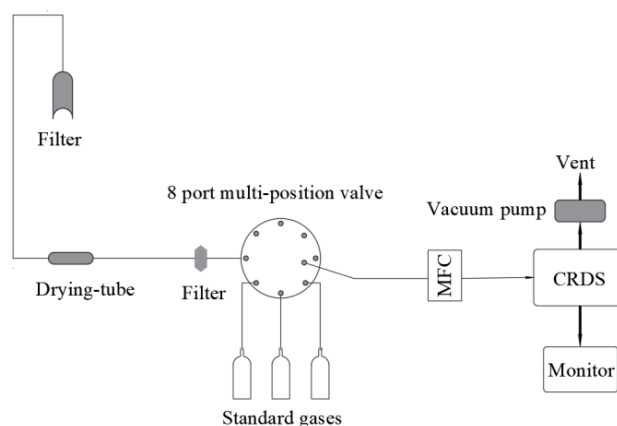


1 2012 (a) and June 2013 (b). Symbols represent the Tae-ahn Peninsula station (TAP, 36.73 °N
2 126.13 °E, 20 m above sea surface), Jeju Gosan station (JGS, 33.30 °N 126.20 °E, 25 m above sea
3 surface) and Lin'an station (LAN, 30.18 °N 119.44 °E, 138 m above sea surface), respectively. ECS
4 represents the East China Sea. The Red Crosses represent the beginning locations of each natural
5 day.

6 2.2 Measurement of atmospheric CO₂ and CH₄ mixing ratios

7 During the field surveys, the air inlet was fixed at the highest point of the bow, about 15 meters
8 from the sea, and near the meteorological sensors to avoid anthropogenic contamination, (Zang et
9 al., 2017). Atmospheric CO₂ and CH₄ mixing ratios were measured using a Picarro system (G2301,
10 Picarro Inc., USA). The Picarro analyzer, which can acquire one measurement every 5 seconds, and
11 correct the measurements influenced by water vapor (Rella et al., 2013), has been proven to be
12 excellent for measuring CO₂ and CH₄ with high precise and accuracy (Crosson, 2008; Fang et al.,
13 2013).

14 Fig. 2 showed the schematic diagram of the CO₂ and CH₄ observation system, ambient air was
15 pumped via the dedicated tube by an external vacuum pump, and passed through a membrane filter
16 (1.0 μm, whatman Inc., USA), a self-assembled drying-tube filled with magnesium perchlorate
17 [Mg(ClO₄)₂] and another filter, respectively, to remove particles and water vapor. Then, regulated
18 by valve sequence setting, dry and clean air sample as well as the standard gases flowed into the
19 CRDS analyzer through 8 port multi-position valve (Valco Instruments Co. Inc. USA) with a flow
20 rate of 200 mL·min⁻¹ controlled by a mass flow controller (Beijing Seven-star electronics Co. LTD.
21 China). Before each campaign, three standard gases were used to calibrate the CRDS analyzer.
22 Linear functions were yielded based on measurement results and the standard values of standard
23 gases, i.e., 254.53 ppm, 365.14 ppm and 569.99 ppm for CO₂, and 1601.0 ppb, 1925.5 ppb and
24 2317.7 ppb for CH₄, respectively. The used standard gases were propagated from the WMO primary
25 standards (WMO/GAW 2004 scale for CH₄, 2007 scale for CO₂), to guarantee the consistency, trace
26 ability and international comparability of observed data (Dlugokencky et al., 2005).



1

2 Fig. 2. Schematic diagram of the shipborne Picarro system for observing atmospheric CO₂ and CH₄.

3 2.3 Meteorological data

4 Both of the two campaigns were conducted by a special designed marine survey ship named
5 “*Dongfanghong IP*”, which was designed and built for multiple disciplines research in marine
6 environment, including a ship-based atmospheric science lab. Meteorological data, including time,
7 latitude, longitude, cruising speed and direction, wind speed, wind direction, relative humidity, air
8 pressure and temperature were observed by the special meteorological sensors with resolution of 10
9 seconds, and were used to filter and flag the observed CO₂ and CH₄ mixing ratios and verify
10 simulated wind fields.

11 2.4 Air mass transport model

12 HYSPLIT (Hybrid Single Particle Lagrangian Integrated Trajectory Model, HYSPLIT) is a
13 model developed by the National Oceanic and Atmospheric Administration's Air Resources
14 Laboratory (NOAA-ARL) and the Bureau of Meteorology of Australia, which can calculate the air
15 mass transportation combined with the National Centers for Environmental Prediction (NCEP)
16 reanalysis data. The principle of simulating the air mass transportation path as follows: assuming
17 that particles in the air are floating in the wind, their moving trajectory is the integral of their position
18 vectors in time and space (Zhang et al., 2011; Xia et al., 2018). Backward trajectory analysis uses
19 the mixed single-particle Lagrangian integral transport and diffusion model to calculate the air
20 particles forward, analyzes the influence of air mass transportation on the spatial and temporal
21 distribution of atmospheric components in the observation area by tracking the transport path, and

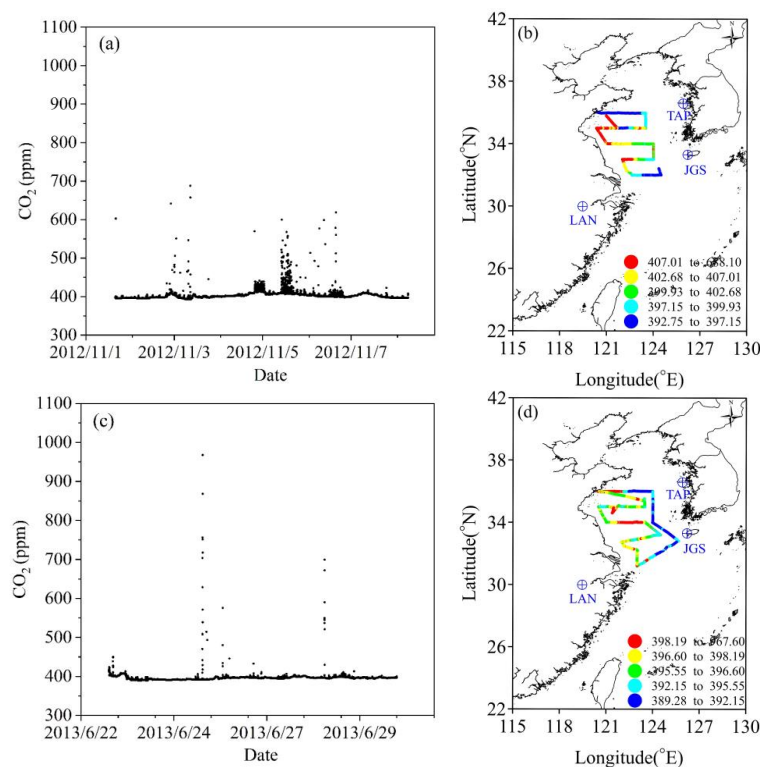


1 infer their potential sources. The main parameters required to calculate the backward trajectory are
2 the altitude, latitude and longitude of the starting point. Generally, the calculation is carried for 3
3 days (72 h) (Zhan et al., 2009; Zhang et al., 2017; Zhang et al., 2019).

4 3 Results

5 3.1 Atmospheric CO₂ mixing ratios

6 During the field surveys, atmospheric CO₂ mixing ratios ranged from 392.75 ppm to 688.10 ppm
7 with an average value of 403.50 ± 13.70 ppm in November 2012 (Fig. 3a and Fig. 3b), and ranged
8 from 389.28 ppm to 967.60 ppm with an average value of 396.40 ± 12.30 ppm in June 2013 (Fig.
9 3c and Fig. 3d), which was consistent with the changing characteristics of the EAM. Seasonal
10 variations were comparable with the typical observation results of the north hemisphere. Abnormal
11 high observation values might be attributed to exhaust gases of ship or anthropogenic interference
12 of analyzer.



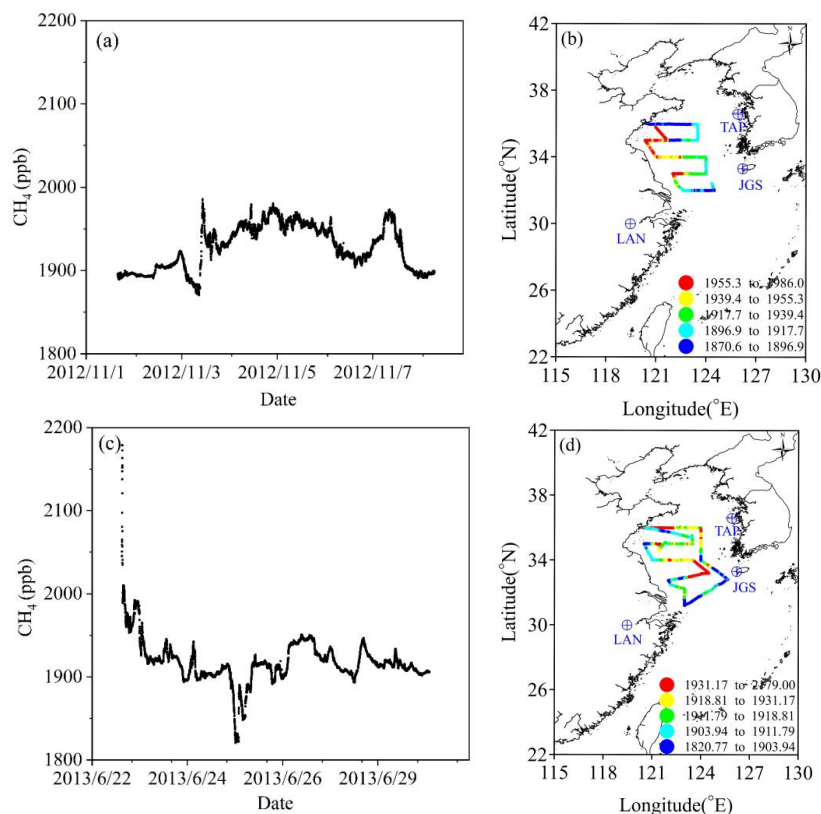
13
14 Fig. 3. Temporal (a and c) and spatial (b and d) distribution of CO₂ mixing ratios in November
15 2012 and June 2013 in the SYS.



1 Our observed mean CO₂ mixing ratios were lower than previous studies' mean values of 405.00
2 ppm and 410.70 ppm in the YS and ECS in March 2013 and March 2017, respectively (Zang et al.,
3 2017; Liu et al., 2018). Moreover, observed mean atmospheric CO₂ mixing ratio was almost equal
4 to results observed at the TAP (401.37 ppm) and JGS (403.77 ppm) stations, but approximate 9 ppm
5 higher than MBL-CO₂ reference (394.41 to 394.78 ppm in latitude zone of 30 °N to 37 °N)
6 (www.esrl.noaa.gov/gmd/ccgg/GHGreference, download data: 2022-10-10) in November 201, and
7 almost equal to results observed at the LAN (396.43 ppm) and JGS (398.10 ppm) stations and MBL-
8 CO₂ reference (397.38 to 397.92 ppm in latitude zone of 30 °N to 37 °N) in June 2013.

9 3.2 Atmospheric CH₄ mixing ratios

10 Atmospheric CH₄ mixing ratios ranged from 1870.6 ppb to 1986.0 ppb with an average value
11 of 1934.1 ± 33.6 ppb in November 2012 (Fig. 4a and Fig. 4b), and ranged from 1820.8 ppb to 2179.0
12 ppb with an average value of 1919.2 ± 30.2 ppb in June 2013 (Fig. 4c and Fig. 4d). Our observed
13 results comparable with observed results at TAP stations, and historical data of 1915.5 ppb in the
14 SYS in March 2013 (Zang et al., 2017), while higher than the MBL-CH₄ references in November
15 2012 (1869.5 to 1880.3 ppb) and June 2013 (1835.3 to 1846.6 ppb).



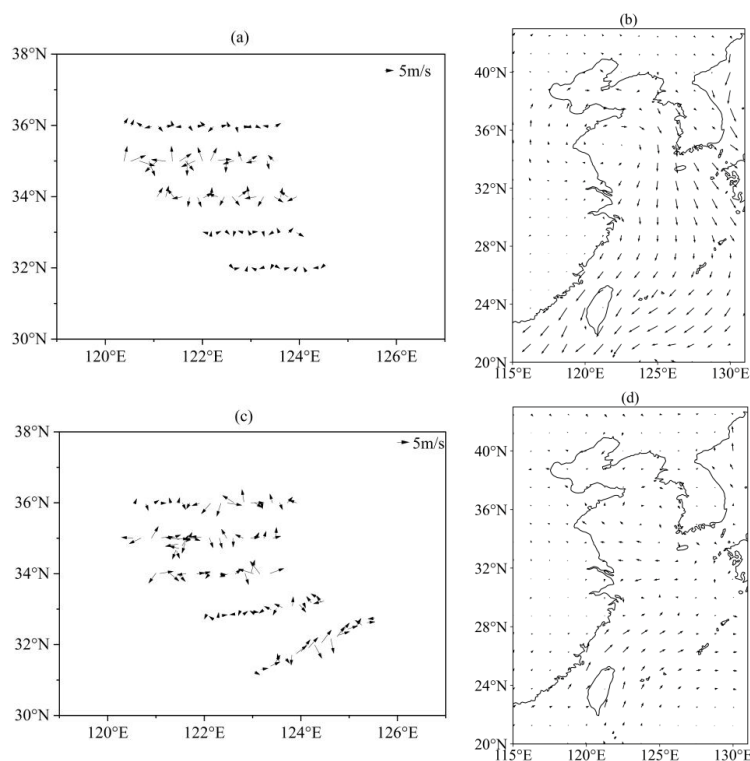
1
2 Fig. 4. Temporal (a and c) and spatial (b and d) distribution of CH₄ mixing ratios in November and
3 June of the SYS.

4 3.3 Wind data

5 Observed wind records were averaged to hourly data for subsequently analysis. As shown in
6 Fig. 5a, during the survey of November 2012, wind speed ranged from 0.05 to 20.46 m/s with an
7 average value of 8.09 ± 4.17 m/s. Dominate wind direction was from north and northeast, indicated
8 the air masses flowed from the Asia continent to the Pacific Ocean. As shown in Fig. 5c, during the
9 survey of June 2013, wind speed ranged from 0.08 m/s to 9.42 m/s with an average value of $4.72 \pm$
10 1.79 m/s. Conversely, the predominant wind direction turned into south or southeast, which
11 promoted air masses flowing from the Pacific Ocean to the Asia continent. In addition, the observed
12 dominant wind directions (Fig. 5a and Fig. 5c) were consisting well with the simulated wind fields
13 (Fig. 5b and Fig. 5d), suggested the typical features of winter and summer monsoon, which were
14 ideal cases to study effects of land-sea air masses transportation on the spatiotemporal variations of



1 CO₂ and CH₄ mixing ratios in the MBL of the SYS.



2
3 Fig. 5. Observed wind direction and speed (a and c) and simulation of wind fields (b and d)
4 over the SYS. The simulated wind fields were plotted based on the ERA5 hourly data on pressure
5 levels provided by the European Centre for Medium-Range Weather Forecasts (ECMWF),
6 (<https://cds.climate.copernicus.eu/cdsapp#!/dataset/reanalysis-era5-pressure-levels?tab=form>,
7 download date: 2022-11-04) and drawn by python 3.7.0.

8 4. Discussion

9 4.1 Optimization of data filter approach

10 Generally, CO₂ and CH₄ mixing ratios decreasing with increasing altitude and distance away
11 from continent, and decreasing latitude (Matsueda et al., 1996; Bartlett et al., 2003; Zang et al.,
12 2017). Spatiotemporal distributions of atmospheric CO₂ and CH₄ mixing ratios in shelf seas read
13 not only natural characteristics, but also multiple anthropogenic processes, such as marine oil and
14 gas exploration (Nara et al., 2014; Zang et al., 2020), land-sea air mass transportation (Kong et al.,
15 2010; Liu et al., 2018) and malfunction of observation instrument (Zang et al., 2017). Although
16 some preliminary data processes have been reported (Zang et al., 2017; Liu et al., 2018), a specific

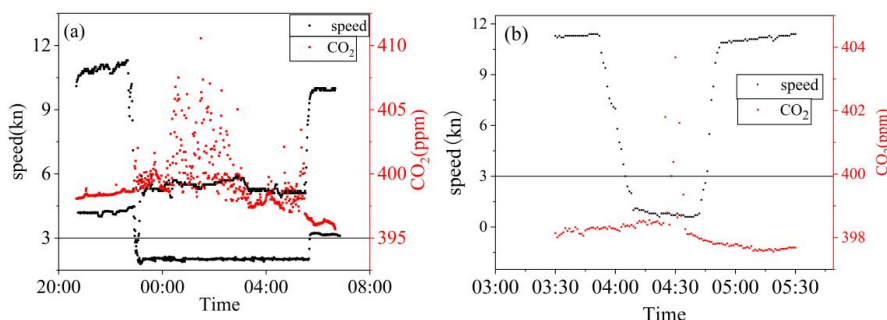


1 data filtering approach for shipborne continuous observation should be optimized to distinguish
2 impacts of diverse source-sink processes on observed CO₂ and CH₄ mixing ratios along the cruise
3 tracks, especially in the shelf seas.

4 Firstly, observed atmospheric CO₂ and CH₄ mixing ratios along the cruise tracks in November
5 2012 and June 2013 were corrected by a linear function, which was established by measurement
6 and propagated values of three CO₂ and CH₄ standard gases. The corrected data were averaged every
7 one minute and named as Raw Data for the subsequently process.

8 Secondly, according to voyage record, the abnormal values that caused by mal-function of
9 instrument or impacted by manual refilling the drying-tube were flagged (Zang et al., 2017).

10 Thirdly, when the ship stopping for sampling at discrete stations or cruising downwind with
11 speed lower than wind speed, observed CO₂ and CH₄ mixing ratios could be impacted by ship's
12 exhaust gas and human activities (Zang et al., 2017; Liu et al., 2018), despite the air inlet was fixed
13 between the chimney and the bow. According to voyage record, previous studies considered 3 knots
14 as the criterion to flag data influenced by ship's exhaust gas and human activities, without statistical
15 analysis (Zang et al., 2017; Liu et al., 2018). For instances, as showed in Fig. 6a and Fig. 6b, when
16 ship speed dropped from normal speed of 11 knots to less than 3 knots, the observed CO₂ mixing
17 ratio varied from a smooth pattern with SD (standard deviation) value less than 0.10 ppm to
18 intensive fluctuation pattern with SD value greater than 1.20 ppm, due to influences of ship
19 emissions and human activities. According to the quality control criteria of CO₂ (SD less than ±
20 0.10 ppm), which recommended by the World Meteorological Organization Global Atmospheric
21 Watch (WMO/GAW), 3 knots was guaranteed as the threshold ship speed. Results showed that, 15.5%
22 and 21.9% of total observed data in November 2012 and June 2013 were flagged as influenced by
23 human activities.

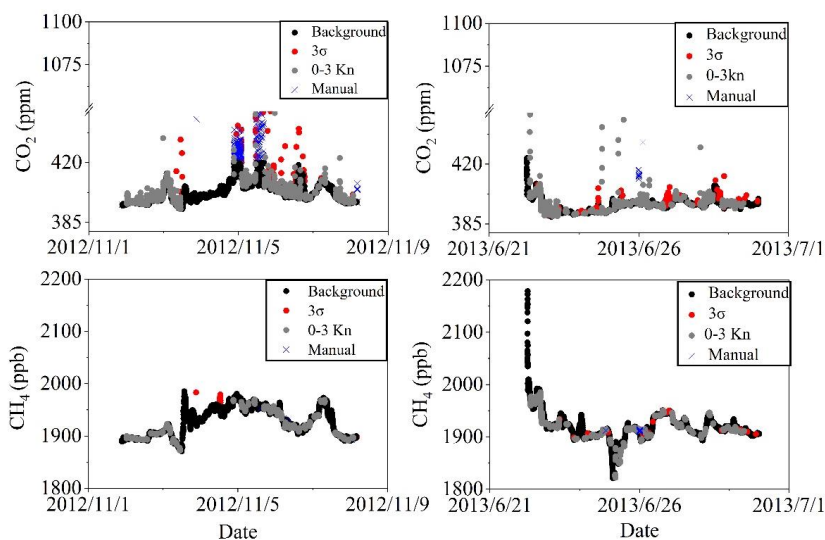


1

2 Fig. 6. Variations of observed CO₂ mixing ratios and ship speed from 20:40 on 28th
3 June 2013 (a) and 3:30 to 5:30 on 3th November 2012(b).

4 Finally, the Pauta criterion (“3 σ ” method), a widely used data quality control approach in
5 atmospheric greenhouse gas observation (Zhang et al., 2013; Fang et al., 2015; Zang et al., 2017),
6 was introduced to filter and flag the non-background observation results. To optimize this process,
7 observation data that covered period of 0.5, 1, 2 and 4 hour was calculated, respectively. Any
8 deviations between observed results and average value lying outside ± 3 SD were considered as
9 non-background data and should be flagged. This procedure was repeated until no outliers were
10 identified (Zhang et al., 2007). Result showed that data calculated hourly by the Pauta criterion was
11 optimal, because it could not only flag dispersed values, but keep the smooth data well.

12 Based on the optimized approach, observed data could be filtered and flagged as shown in Fig.
13 7, the remained data accounted for 79.5% and 75.7% of original data in November 2012 and June
14 2013, respectively, which were considered as background data, and used for further analysis.



1
2 Fig. 7. Filtered results of CO₂ (a, b) and CH₄ (c, d) mixing ratios in November 2012 and June 2013,
3 the ordinates of a and b are truncated in the range of 450 to 1050 ppm. Black points represent the
4 background data (Background), the red points represent the data filtered out by the Pauta criterion
5 (3σ), the green points mean the data influenced by ship emissions at low speed (0-3 Kn), and the
6 blue crosses indicate unreasonable data that were manually screened (Manual).

7 4.2 Influence of air-sea exchange on distribution of atmospheric CO₂ and CH₄ mixing ratios

8 Air-sea exchange is a dynamic process when CO₂ and CH₄ molecules diffusing between the
9 interface of surface seawater and overlying atmosphere. Source and sink of atmospheric CO₂ and
10 CH₄ mean they were emitted from or absorbed by seawater. In fact, the magnitude of air - sea CO₂
11 and CH₄ exchange varied dramatically in spatial and temporal scale in coastal seas (Yang et al., 2016;
12 Gao et al., 2019). Generally, CO₂ and CH₄ emitted from the seawater into the air were difficult to
13 trace by atmospheric measurements because they could dilute sharply (Schmale et al., 2005;
14 Kourtidis et al., 2006; Zhai et al., 2013), only shallow seeps areas and coastal regions, could
15 influence the mixing ratios of local atmospheric CO₂ and CH₄ directly and be measured (Leifer et
16 al., 2006; Luo et al., 2015). Despite the dissolved CO₂ and CH₄ were not observed in our field
17 surveys, the published data showed that sea-to-air CO₂ fluxes were 6.0 ± 8.8 mmol/m²/day in
18 November 2012 and 2.6 ± 4.3 mmol/m²/day in June 2011 (Wang and Zhai, 2021), and sea-to-air
19 CH₄ fluxes were 6.4 μ mol/m²/day in November 2002 and 15.7 μ mol/m²/day in June 2006 (Zhang



1 et al., 2008), respectively, in the SYS.

2 To estimate the effects of air-sea exchange on mixing ratios of atmospheric CO₂ and CH₄, we
3 used a simple method described by Kourtidis et al. (2006) and optimized by Zang et al. (2020):
4 assumed that a box located above the survey area, with a ceiling of 10 meters which corresponding
5 to the height of air inlet in our field surveys. The contents of atmospheric CO₂ and CH₄ were only
6 impacted by air-sea exchange. When CO₂ and CH₄ were vented into or absorbed from the box, their
7 mixing ratios would increase or decrease homogeneously, caused by the mean calculated results of
8 sea-to-air CO₂ and CH₄ fluxes.

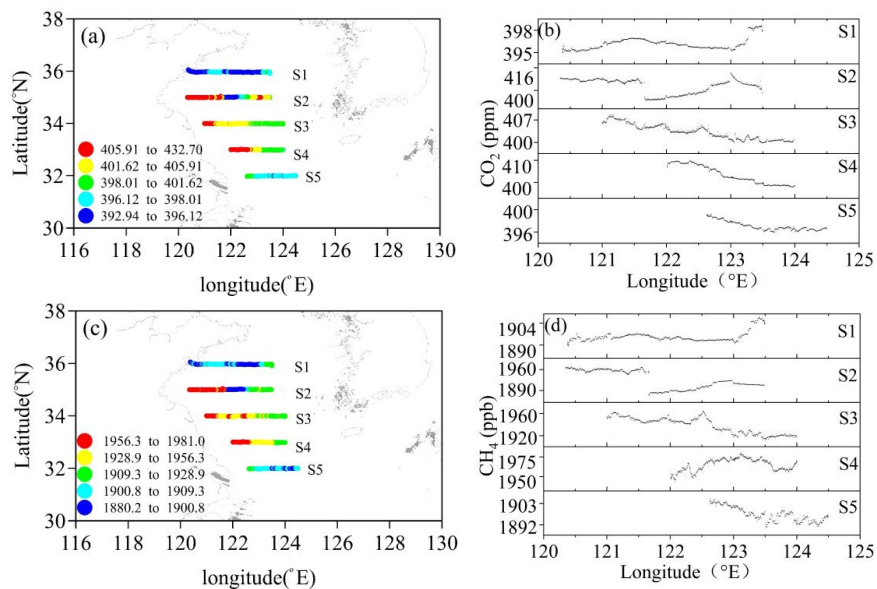
9 For CH₄, generally, coastal shallow seas are source of atmospheric CH₄, accounting for
10 approximate 75% of global ocean emissions (Bange et al., 1994; Bates et al., 1996). However,
11 according to the calculation formula that given by Zang et al. (2020), sea-to-air CH₄ flux of 50.8
12 μmol/m²/day would result in an increasing of 2 ppb of atmospheric CH₄ mixing ratio in the MBL.
13 Thus, the impacts of the reported mean sea-to-air CH₄ fluxes (6.4 μmol/m²/day and 15.7
14 μmol/m²/day in November 2002 and June 2006) on the atmospheric CH₄ would not exceed 1 ppb
15 (Zhang et al., 2008). In addition, based on the same method, we calculated the impacts of the
16 reported mean sea-to-air CO₂ fluxes (Wang and Zhai, 2021) on the atmospheric CO₂ mixing ratios
17 was no more than 14.1 ppb. Thus, it was reasonable to conclude that influences of air-sea exchange
18 on distribution of atmospheric CO₂ and CH₄ mixing ratios were negligible, compared to the
19 observed variability of atmospheric CH₄ (Fig.3 and Fig. 4).

20 4.3 Influences of land-sea air mass transportation on spatiotemporal distribution of atmospheric
21 CO₂ and CH₄ mixing ratios

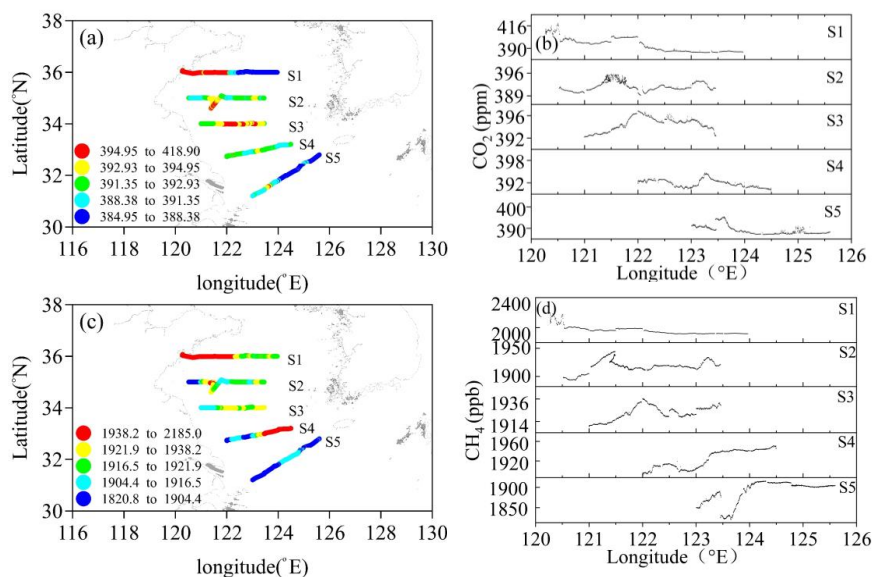
22 The EAWM is closely related to atmospheric compounds transportation from the Asia
23 continent to the Western Pacific (Yu et al., 2014). Since two surveys were conducted in November
24 2012 and June 2013, when the typical winter and summer monsoon season in their early phases,
25 respectively (Lyu et al., 2021; Lin'an et al., 2022), the observation data could give us an ideal
26 opportunity to study the impacts of land-to-sea air mass transportation on spatiotemporal
27 distribution of atmospheric CO₂ and CH₄ mixing ratios over the SYS. The observed atmospheric
28 CO₂ and CH₄ mixing ratios were higher in November 2012 (Fig. 8) than that in July 2013 (Fig. 9).
29 Except for the Section 1 (S1) and the right end of Section 2 (S2), the spatial distributions were



1 gradient with offshore distance (Fig. 8).
2 In situ observed data demonstrated that the dominant wind direction was W-NW-NNW for section
3 2, 3, 4 and 5 in November 2012, suggested the air masses were transported from the Asian Continent
4 to the Pacific Ocean (Fig. 5 and Supplementary data). Generally, CO₂ and CH₄ mixing ratios were
5 higher in continent than that of the MBL, land-to-sea air mass transportation driven by the EAWM
6 could result in the horizontal transmission of greenhouse gases (Zhang et al., 2007; Zang et al., 2017;
7 Liu et al., 2018). Due to the subsequently mixing, CO₂ and CH₄ mixing ratios would decline along
8 the windward (Bartlett et al., 2003; Kourtidis et al., 2006; Liu et al., 2018). Meanwhile, the mixing
9 ratios of atmosphere CO₂ and CH₄ were low and homogeneous in Section 1 and right end of Section
10 2, because the dominant wind direction was ENE-SE-S, indicated air masses were transported from
11 the open Pacific Ocean with low content of CO₂ and CH₄, because of weak human activities
12 (Matsuda, 1996; Bartlett et al., 2003; Zang et al., 2017).



13
14 Fig. 8. Spatial distributions of CO₂ and CH₄ mixing ratios in the survey area in November
15 2012.



1

2

Fig. 9. Spatial distributions of CO₂ and CH₄ mixing ratios in the survey area in July 2013.

3

4

5

6

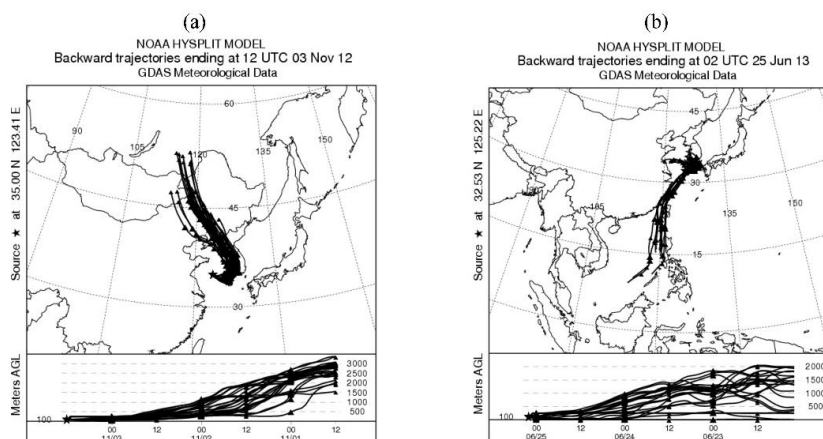
7

8

9

10

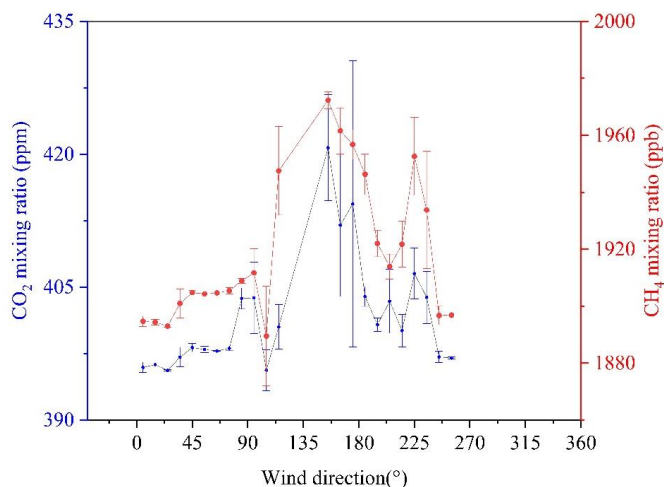
Furthermore, back trajectory analysis showed that almost all the transport track were originated from the Asian Continent in November 2012, and the South China Sea and West Pacific Ocean in July 2013 (typical characteristics of the early summer monsoon) (Fig. 10), which resulted in higher atmospheric CO₂ and CH₄ mixing ratios in November 2012 (Fig. 8) than that in July 2013 (Fig. 9). Seasonal variations of atmospheric CO₂ and CH₄ mixing ratios were consistent with the variations of atmospheric CO₂ mixing ratios in West Pacific Ocean, where atmospheric components distributions were dominated by maritime air masses from the Pacific Ocean and polluted air masses from the Asian Continent (Matsuda, 1996; Zhang et al., 2007).



1
2 Fig. 10. Three-day air back-trajectories of two typical locations, a (35.00 °N, 123.41 °E) and b
3 (32.53 °N, 125.22 °E).

4 4.4 Estimated distance of air mass transportation

5 As shown in Fig. 11, atmospheric CO₂ and CH₄ mixing ratios fluctuated in the same phase
6 along with wind direction, indicated their variations were dominated by the same emission and air
7 masses transportation, which was in agreement with previous studies (Zang et al., 2017; 2020).

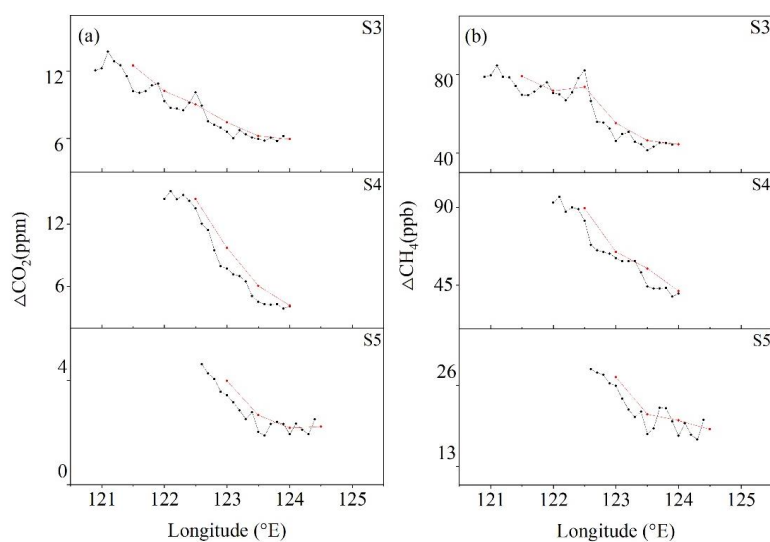


8
9 Fig. 11. Atmospheric mixing ratios of CO₂ and CH₄ as a function of wind direction. Error bars
10 indicate two standard errors within each wind direction bin.

11 Simulation studies of gas seeps in the Black Sea and the Nord Stream pipeline gas leaks in the



1 Baltic Sea showed that atmospheric CH₄ mixing ratio could be enhanced by the upwind emission
2 source in distance of 5 to 30 km (Kourtidis et al., 2006; Jia et al., 2022). NOAA's MBL-CO₂ and
3 MBL-CH₄ values were 394.56 ppm and 1875.4 ppb, respectively, at the same latitude zone with the
4 survey area in November 2012. ΔCO_2 and ΔCH_4 represented deviations between observed
5 atmospheric CO₂ and CH₄ mixing ratios and MBL-CO₂ and MBL-CH₄ references. As shown in Fig.
6 12, we assumed that the effects of mixing and dilution during the transportation was linear
7 (Kourtidis et al., 2006), the further the observation site away from continent, the lower the ΔCO_2
8 and ΔCH_4 values in each survey section. According to the calculated slope values, the inflection
9 points of gradient could be set at 123.30 °E, 123.50 °E and 123.40 °E for section 3, 4 and 5,
10 respectively. Moreover, the offshore distances away from continent could be calculated as
11 approximate 27.0, 26.3 and 11.7 km, respectively, with a mean value of 21.7 km. Thus, spatial
12 distributions of atmospheric CO₂ and CH₄ mixing ratios in the China shelf sea could be impacted
13 remarkably by land-to-sea air mass transportation during early phase of the EAWM.



14
15 Fig. 12. The average value of ΔCO_2 (a) and ΔCH_4 (b) per 0.1 (black) or 0.5 longitude (red).

16 5. Conclusions

17 Based on the continuous observed CO₂ and CH₄ mixing ratios and meteorological parameters
18 over the south Yellow Sea in November 2012 and June 2013, a data filter method was optimized
19 and established, which could be used to flag CO₂ and CH₄ mixing ratios influenced by diverse



1 natural and human activities. Spatial and seasonal variations of atmospheric CO₂ and CH₄ mixing
2 ratios over the SYS were mainly regulated by the EAM, while the influence of air-sea exchange was
3 slight or negligible. Summer monsoon resulted in relatively low atmospheric CO₂ and CH₄ mixing
4 ratios with a gradient increasing from southeast to northwest. Conversely, winter monsoon enhanced
5 land-to-sea air masses transportation with high CO₂ and CH₄ mixing ratios, which induced
6 decreasing patterns with increasing distance offshore. Effect of land-to-sea air mass transportation
7 on enhanced CO₂ and CH₄ mixing ratios was assessed as a distance of approximate 20 km offshore
8 in the early period of the EAWM.

9

10 *Code availability.* The code that is used for figure plotting (python) can be provided upon
11 request.

12 *Data availability.* The ERA5 hourly data on pressure levels provided by the European Centre
13 for Medium-Range Weather Forecasts (ECMWF),
14 <https://cds.climate.copernicus.eu/cdsapp#!/dataset/reanalysis-era5-pressure-levels?tab=form>,
15 download date: 2022-11-04). The simulated MBL values produced by NOAA,
16 www.esrl.noaa.gov/gmd/ccgg/GHGreference, download data: 2022-10-10.

17 **Author contributions**

18 Li jiaxin prepared the main part of the paper and performed the corresponding analyses. Zang
19 Kunpeng provided the original data that are used within this study and helped with the data analyses
20 and the preparation of the paper. Lin Yi, Chen Yuanyuan and Liu Shuo provided valuable comments
21 on data processing and, as well as help in the drawing of Fig. 5. Fang Shuangxi, Qiu Shanshan and
22 Jiang kai suggestions for revising the paper and further standardized the paper. Xiong Haoyu, Qing
23 Xuemei and Hong Haixiang helped download the MBL data required for the article.

24 **Competing interest**

25 This manuscript is approved by all authors for publication, and we have no competing interests
26 to declare that are relevant to the content of this article.

27 **Acknowledgments**

28 The authors wish to thank the crew of the R/V “Dongfanghong II” for their assistance on board.



1 This work was supported by the National Key Research and Development Program of China
2 (2020YFA0607501), the National Natural Science Foundation of China (No. 42275113), the Special
3 Support Plan for High-level Talents in Zhejiang province (2021R542048), the Joint funds of the
4 Zhejiang Provincial Natural Science Foundation of China under Grant No. LZJMZ23D050002, the
5 Fund of Key Laboratory of Global Change and Marine-Atmospheric Chemistry, MNR
6 (GCMAC2001) and the Basic Public Welfare Research Program of Zhejiang Province
7 (LGF22D050004).



1 **References**

- 2 AGGI. The NOAA annual greenhouse gas index (AGGI). NOAA Earth System Research Laboratory, Boulder,
3 Colorado, USA. <http://esrl.noaa.gov/gmd/aggi/aggi.html>, 2014.
- 4 Bange, H. W., Bartell, U. H., Rapsomanikis, S., and Andre, M. O.: Methane in the Baltic and North Seas and a
5 Reassessment of the Marine Emissions of Methane, *Global Biogeochem Cy.*, 8, 465-480,
6 <https://doi.org/10.1016/j.marchem.2008.02.005>, 1994.
- 7 Bartlett, K. B., Sachse, G. W., Slate, T., Harward, C., and Blake, D. R.: Large-scale distribution of CH₄ in the
8 western North Pacific: Sources and transport from the Asian continent, *J. Geophys. Res-Atmos.*, 108, D20,
9 <https://doi:10.1029/2002JD003076>, 2003.
- 10 Bouman, E. A., Lindstad, E., Riialand, A. I., and Stomman, A. H.: State-of-the-art technologies, measures, and
11 potential for reducing GHG emissions from shipping-A review, *Transport. Res. D-Tr. E*, 52, 408-421,
12 <http://dx.doi.org/10.1016/j.trd.2017.03.022>, 2017.
- 13 Chang, C., L. Yi, and Chen, G. T.: A numerical simulation of vortex development during the 1992 east Asian
14 summer monsoon onset using the navy's regional model, *Mon. Wea. Rev.*, 128, 1604–1631,
15 [https://doi.org/10.1175/1520-0493\(2000\)128<1604:ANSOVD>2.0.CO;2](https://doi.org/10.1175/1520-0493(2000)128<1604:ANSOVD>2.0.CO;2), 2000.
- 16 Crosson, E. R.: A cavity ring-down analyzer for measuring atmospheric levels of methane, carbon dioxide, and
17 water vapor, *App. Phys. B-Lasers. O.*, 92, 403-408, <https://10.1007/s00340-008-3135-y>, 2008.
- 18 Dlugokencky, E. J., Myers, R. C., Lang, P. M., Masarie, K. A., Crotwell, A. M., Thoning, K. W., Hall, B. D.,
19 Elkins, J. W., and Steele, L. P.: Conversion of NOAA atmospheric dry air CH₄ mole fractions to a gravimetrically
20 prepared standard scale, *J. Geophys. Res.*, 110, D18306, <https://doi.org/10.1029/2005JD006035>, 2005.
- 21 Ding, Y. H., Liu, J. J., Sun, Y., Liu, Y., He, J., and Song, Y.: A study of the synoptic-climatology of the Meiyu
22 system in East Asia, *Chinese Journal of Atmospheric Sciences*, 31, 1082-1101, 2007.
- 23 Ding, J., Van Der A, R. J., Mijling, B., Jalkanen, J. P., Johansson, L., and Levelt, P. F.: Maritime NO_x emissions
24 over Chinese Seas derived from satellite observations, *Geophys. Res. Lett.*, 45, 2031-2037,
25 <https://doi.org/10.1002/2017GL076788>, 2018.
- 26 Fang, S. X., Zhou, L. X., Masarie, K. A., Xu, L., and Rella, C. W.: Study of atmospheric CH₄ mole fractions at
27 three WMO/GAW stations in China, *J. Geophys. Res-Atmos.*, 118, 4874-4886, <https://doi.org/10.1002/jgrd.50284>,
28 2013.
- 29 Fang, S. X., Tans, P. P., Steinbacher, M., Zhou, L. X., and Luan, T.: Comparison of the regional CO₂ mole



- 1 fraction filtering approaches at a WMO/GAW regional station in China, *Atmos. Meas. Tech.*, 8, 5301-5313,
2 <https://doi.org/10.5194/amt-8-5301-2015>, 2015.
- 3 Gao, Z. M., Liu, H. P., and Mcfarland, D. P.: Mechanistic links between underestimated CO₂ fluxes and non-
4 closure of the surface energy balance in a semi-arid sagebrush ecosystem, *Enviro. Res. Lett.*, 14, 1748-9326,
5 <https://doi.org/10.1088/1748-9326/ab82d>, 2019.
- 6 Huang, R. H.: The influence of the heat source anomaly over Tibetan Plateau on the northern hemispheric
7 circulation anomalies, *Acta Meteorol Sin.*, 43, 208-220, 1985.
- 8 Houghton, R. H., Zhou, L. T., and Chen, W.: The progresses of recent studies on the variabilities of the East
9 Asian monsoon and their causes, *Adv. Atmos. Sci.*, 20, 55-69, 2003.
- 10 Jia, M., Li, F., Zhang, Y. Z., Wu, M. S., Li, Y. S., Feng, S. Z., Wang, H. M., Chen, H. L., Ju, W. M., Lin, J., Cai,
11 J. W., Zhang, Y. G., and Jiang, F.: The Nord Stream pipeline gas leaks released approximately 220,000 tonnes of
12 methane into the atmosphere, *Environmental Science and Ecotechnology*, 12, 2666-4984, [https://](https://doi.org/10.1016/j.ese.2022.100210)
13 doi.org/10.1016/j.ese.2022.100210, 2022.
- 14 Kourtidis, K., Kioutsioukis, I., McGinnis, D. F., and Rapsomanikis, S.: Effects of methane outgassing on the
15 Black Sea atmosphere, *Atmos. Chem. Phys.*, 6, 5173–5182, <https://doi.org/10.5194/acp-6-5173-2006>, 2006.
- 16 Kong, S., Lu, B., Han, B., Bai, Z. P., Xu, Z., You, Y., Jin, L. M., Guo, X. Y., and Wang, R.: Seasonal variation
17 analysis of atmospheric CH₄, N₂O and CO₂ in Tianjin offshore area. *Sci. China Earth Sci.*, 53, 1205–1215, [https://](https://doi.org/10.1007/s11430-010-3065-5)
18 [doi: 10.1007/s11430-010-3065-5](https://doi.org/10.1007/s11430-010-3065-5), 2010.
- 19 Law, C. S., Brévière, E., De Leeuw, G., Garçon, V., Guieu, C., Kieber, D. J., Konradowitz, S., Paulmier, A.,
20 Quinn, P. K., Saltzman, E. S., Stefels, J., and Von Glasow, R.: Evolving research directions in Surface Ocean-Lower
21 Atmosphere (SOLAS) science, *Environ. Chem.*, 10, 1-16, <https://doi.org/10.1071/EN12159>, 2013.
- 22 Luo, X. F., Wei, H., Liu, Z., and Zhao, L.: Seasonal variability of air–sea CO₂ fluxes in the Yellow and East
23 China Seas: A case study of continental shelf sea carbon cycle model, *Cont. Shelf. Res.*, 107, 69-78,
24 <http://dx.doi.org/10.1016/j.csr.2015.07.009>, 2015.
- 25 Liu, Y. S., Zhou, L. X., Tans, P. P., Zang, K. P., and Cheng, S. Y.: Ratios of greenhouse gas emissions observed
26 over the Yellow Sea and the East China Sea, *Sci. Total. Environ.*, 33, 1022-1031
27 <https://doi.org/10.1016/j.scitotenv.2018.03.250>, 2018.
- 28 Lyu, W. Z., Fu, T. F., Hu, Z. X., Tang, Y. Z., Chen, G. Q., Xu, X. Y., Chen, Y. P., and Chen, S. L.: Sedimentary
29 dynamics of the central South Yellow Sea revealing the relation between east asian Summer and Winter Monsoon



- 1 over the past 6000 years, *Front. Earth Sci.*, 9, 689508, <https://doi.org/10.3389/feart.2021.689508>, 2021.
- 2 Masarie, K. A., and Tans, P. P. Extension and integration of atmospheric carbon-dioxide data into a globally
3 consistent measurement record. *J. Geophys. Res.-Atmos.*, 100, 11593-11610, <https://doi.org/10.1029/95JD00859>,
4 1995.
- 5 Matsueda, H., Inoue, H. Y., Ishii, M., and Nogi, Y.: Atmospheric methane over the North Pacific from 1987 to
6 1993. *Geochem. J.*, 30, 1-15, 1996.
- 7 Nara, H., Tanimoto, H., Tohjima, Y., Mukai, H., Nojiri, Y., and Machida, T.: Emissions of methane from offshore
8 oil and gas platforms in Southeast Asia, *Sci Rep* 4, 6503, <https://doi.org/10.1038/srep06503>, 2014.
- 9 Peters, G., Marland, G., Le Quééré, C., Boden, T., Canadell, J. G., and Raupach, M. R.: Rapid growth in CO₂
10 emissions after the 2008-2009 global financial crisis, *Nat. Clim. Change.*, 2, 2-4,
11 <https://doi.org/10.1038/nclimate1332>, 2012.
- 12 Rella, C. W., Chen, H., Andrews, A. E., Filges, A., Gerbig, C., Hatakka, J., Karion, A., Miles, N. L., Richardson,
13 S. J., Steinbacher, M., Sweeney, C., Wastine, B., and Zellweger, C.: High accuracy measurements of dry mole
14 fractions of carbon dioxide and methane in humid air, *Atmos. Meas. Tech.*, 6, 837-860, [https://doi.org/10.5194/amt-](https://doi.org/10.5194/amt-6-837-2013)
15 [6-837-2013](https://doi.org/10.5194/amt-6-837-2013), 2013.
- 16 Riddick, S. N., Mauzerall, D. L., Cella, M., Harris, N. R. P., Allen, G., Pitt, J., Staunton-Sykes, J., Forster, G.
17 L., Kang, M., Lowry, D., Nisbet, E. G., and Manning, A. J.: Methane emission from oil and gas platforms in the
18 North Sea. *Atmos. Chem. Phys.*, 19, 9787-9796, <https://doi.org/10.5194/acp-19-9787-2019>, 2019.
- 19 Schmale, O., Greinert, J., and Rehde, R. G.: Methane emission from high-intensity marine gas seeps in the Black
20 Sea into the atmosphere, *Geophys. Res. Lett.*, 32, 7, <https://doi.org/10.1029/2004GL021138> (2005).
- 21 Warneke, T., De Beek, R., Buchwitz, M., Notholt, J., Schulz, A., Velasco, V., and Schrems, O.: Shipborne
22 solar absorption measurements of CO₂, CH₄, N₂O and CO and comparison with SCIAMACHY WFM-DOAS
23 retrievals, *Atmos. Chem. Phys.*, 5, 2029-2034, <https://doi.org/10.5194/acp-5-2029-2005>, 2005.
- 24 Wang, S. Y., and Zhai, W. D.: Regional differences in seasonal variation of air-sea CO₂ exchange in the Yellow
25 Sea. *Cont. Shelf. Res.*, 218, 104393, <https://doi.org/10.1016/j.csr.2021.104393>, 2021.
- 26 WMO. Greenhouse Gas Bulletin: The state of greenhouse gases in the atmosphere based on global observations
27 through 2021. <http://www.wmo.int/pages/prog/arep/gaw/ghg/ghgbull06en.html>, 2022.
- 28 XIA, L. J., Liu, L. X., Li, B. Z., and Zhou, L. X.: Spatial and temporal distribution characteristics of atmospheric
29 CO₂ in central China, *China Environmental Science*, 38, 2811-2819, [23](https://doi.org/10.19674/j.cnki.issn1000-</p></div><div data-bbox=)



- 1 [6923.2018.0294](https://doi.org/10.5194/amt-2023-3), 2018.
- 2 Yu, G., Chen, Z., Piao, S. L., Peng, C. H., Ciais, P., Wang, Q. F., Li, X. R., and Zhu, X. J.: High carbon dioxide
3 uptake by subtropical forest ecosystems in the East Asian monsoon region. *Proc. Natl. Acad. Sci. U. S.*, 111, 4910-
4 4915, <https://doi.org/10.1073/pnas.1317065111>, 2014.
- 5 Yang, M., Bell, T. G., Hopkins, F. E., Kitidis, V., Cazenave, P. W., Nightingale, P. D., Yelland, M. J., Pascal,
6 R. W., Prytherch, J., Brooks, I. M., and Smyth, T. J.: Air-sea fluxes of CO₂ and CH₄ from the Penlee Point
7 Atmospheric Observatory on the south-west coast of the UK, *Atmos. Chem. Phys.*, 16, 5745–5761,
8 <https://doi.org/10.5194/acp-16-5745-2016>, 2016.
- 9 Zhan, L. Y., and Chen, L. Q.: Distribution characteristics of atmospheric nitrous oxide in the Southern Ocean,
10 *Chinese Journal of Polar Research*, 2007, 49-60, 2007.
- 11 Zhan, R. F., and Li, J. P.: Influence of atmospheric heat sources over the Tibetan Plateau and the tropical
12 western North Pacific on the inter-decadal variations of the stratosphere-troposphere exchange of water vapor, *Sci.*
13 *China Ser. D-Earth Sci.*, 51, 1179-1193, <https://doi.org/10.1007/s11430-008-0082-8>, 2008.
- 14 Zhang, G. L., Zhang, J., Ren, J. L., Li, J. B., and Liu, S. M.: Distributions and sea-to-air fluxes of methane and
15 nitrous oxide in the North East China Sea in summer, *Mar. Chem.*, 110, 42-55,
16 <https://doi.org/10.1016/j.marchem.2008.02.005>, 2008.
- 17 Zhan, M. J., Sun, J. Y., Zhang, Y. M., Zhang, X. C., Nie, H., Deligeer, Kivekas, N., and Lihavainen, H.: The
18 influence of air mass sources on the particle number concentration and the size distribution at Mt. Waliguan, *Journal*
19 *of Glaciology and Geocryology*, 31, 659-663, 2009.
- 20 Zang, K. P., Zhao, H. D., Wang, J. Y., Xu, X. M., Huo, C., and Zheng, N.: High-resolution measurement of
21 CH₄ in sea surface air based on cavity ring-down spectroscopy technique: the first trial in China Seas. *Acta Scientiae*
22 *Circumstantiae*, 33, 1362-1366, 2013.
- 23 Zhang, F., Chen, Y. J., Tian, C. G., Wang, X. P., Huang, G. P., Fang, Y., and Zong, Zheng.: Identification and
24 quantification of shipping emissions in Bohai Rim, China, *Sci Total Environ*, 497-498, 570-577,
25 <https://doi.org/10.1016/j.scitotenv.2014.08.016>, 2014.
- 26 Zhai, W. D.: Sea surface partial pressure of CO₂ and its controls in the northern south China Sea in the non-
27 bloom period in spring, *Haiyang Xuebao*, 37, 31-40, <https://doi.org/10.3969/j.issn.0253-4193.2015.06.004>, 2015.
- 28 Zhang, J. Y., Song, S. H., Xu, R., and Wen, J. H.: Source of airborne particulate matter in Guilin based on
29 backward trajectory model, *Environmental Monitoring in China*, 33, 42-46, <https://doi.org/10.19316/j.issn.1002->



- 1 6002.2017.02.07, 2017.
- 2 Zang, K. P., Zhou, L. X., and Wang, J. Y.: Carbon Dioxide and Methane in the China Sea Shelf Boundary
3 Layer observed by Cavity Ring-Down Spectroscopy, *J. Atmos. and Ocean. Tech.*, 34, 2233-2244,
4 <https://doi.org/10.1175/JTECH-D-16-0217.1>, 2017.
- 5 Zhang, Z. P., and Chu, Z. X.: Modern variations in clay minerals in mud deposits of the Yellow and East China
6 Seas and their geological significance, *Holocene* 28, 386-395 <https://doi.org/10.1177/0959683617729446>, 2018.
- 7 Zou, L., Hu, B., Li, J., Dou, Y. G., Xie, L. H., and Dong, L.: Middle Holocene Organic Carbon and biomarker
8 records from the South Yellow Sea: relationship to the East Asian Monsoon, *J. Ocean Univ. China*, 17, 823-834,
9 <https://doi.org/10.1007/s11802-018-3521-y>, 2018.
- 10 Zhang, Y., Deng, F., Man, H., Fu, M., Lv, Z., Xiao, Q., Jin, X., Liu, S., He, K., and Liu, H.: Compliance and
11 port air quality features with respect to ship fuel switching regulation: a field observation campaign, SEISO-Bohai,
12 *Atmos. Chem. Phys.*, 19, 4899–4916, <https://doi.org/10.5194/acp-19-4899-2019>, 2019.
- 13 Zang, K. P., Zhang, G., Xu, X. M., and Yao, Z. W.: Impact of air-sea exchange on the spatial distribution of
14 atmospheric methane in the Dalian Bay and adjacent coastal area, China, *Chemosphere*, 251, 126412,
15 <https://doi.org/10.1016/j.chemosphere.2020.126412>, 2020.
- 16



1 **Author biography**



2

3 **Kunpeng Zang**

4 Education experience:

5 2003-2007 Nanjing University of Information Science and Technology,
6 undergraduate.

7 2007-2010 Chinese Academy of Meteorological Sciences, environmental
8 engineering, Master.

9 2014-2018 Nanjing University of Information Science and Technology,
10 Atmospheric Physics and Atmospheric Environment, Doctor.

11 Working experience:

12 2010-2020 National Marine Environmental Monitoring Center.

13 2020-now Zhejiang University of Technology, Lecturer.

14 Research field:

15 Greenhouse Gas observation research.

16



17

18 **Shuangxi Fang**

19 Education experience:

20 1998-2003 Wuhan University, undergraduate.



1 2002-2007 Institute of Ecology and Environment, Chinese Academy of Sciences,
2 Master Degree Candidate and Doctor.

3 Working experience:

4 2007-2015 Chinese Academy of Meteorological Sciences.

5 2015-2019 Meteorological Observation Center of China Meteorological
6 Administration.

7 2019-now Zhejiang University of Technology, Professor.

8 2021-now Zhejiang Carbon Neutral Innovation Institute, Dean.

9 Research field:

10 Greenhouse Gas observation research.

11



12

13 **Jiaxin Li**

14 Education experience:

15 2016-2020 Heilongjiang University of Science and Technology, environmental
16 engineering, undergraduate.

17 2020-2023 Zhejiang University of Technology, Master.

18 Research field:

19 Greenhouse Gas observation research.